Pergamon

0045-7949(94)00494-3

Computers & Structures Vol. 55, No. 4, pp. 659–666, 1995

0045-7949/95 $9.50 + 0.00

THE FINITE ELEMENT METHOD OF THREE-DIMENSIONAL NONLINEAR VISCOELASTIC LARGE DEFORMATION PROBLEMS

Y. P. Shen,† N. Hasebe‡ and L. X. Lee†
†Xi'an Jiaotong University, Xi'an 710049, People's Republic of China
‡Nagoya Institute of Technology, Nagoya 466, Japan

(*Received* 10 *November* 1993)

Abstract—The nonlinear viscoelastic large deformation incremental variational equations based on the T.L. and U.L. approaches are derived. The finite element formulation and solution procedure are developed for three-dimensional problems. Compared to the U.L. approach, the T.L. approach is simple and saves computer time. The computational results of a nonlinear viscoelastic large deformation cantilever and a hollow thick viscoelastic cylinder with a steel casing are in reasonable agreement with Yang and Lianis [*J. Appl. Mech.* **41,** 635–640 (1974)] and Shen *et al.*, *Comput. Struct. Mech. Appl.* **2,** 43–54 (1987), in Chinese], and the effects of material incompressibility on stress analysis are discussed.

1. INTRODUCTION

Owing to the extensive application of polymers, and along with an increasing demand for work reliability for rocket solid propellants, the researches on stress and strain of the viscoelastic solid have been impelled to develop rapidly.

For viscoelastic problems of complex geometric shape and loading situation, the finite element method is one of the most effective approaches. Since 1965, a lot of papers have been published. They can be divided into two kinds:

(1) The first kind which includes most of the papers, is where the problems are solved directly in the time domain by use of an incremental step-by-step process. Using linear integral and differential constitutive relations, Zienkiewicz *et al.* [1, 2], White [3], Argyris *et al.* [4] and Srinatha and Lewis [5] compile the finite element programs of stress analysis for two-dimensional plane and axisymmetric viscoelastic solids. The computational results are in good agreement with the analytic solution.

(2) The second kind is that, by use of elasticity–viscoelasticity correspondence, principle viscoelastic problems are translated into elastic problems in Laplace domain, then the elastic problems are solved by the finite element method. After that, by applying the inverse Laplace technique, the solution of the initial viscoelastic problems can be obtained. According to this method, Adey and Brebbia [6] analysed a hollow thick viscoelastic cylinder with a steel casing under uniform internal pressure.

However, all of the above-mentioned papers concern only the two-dimensional linear viscoelastic small deformation problems.

As for viscoelastic large deformation problems, until 1974 approximate and numerical solutions were only obtained for simple one-dimensional linear viscoelastic problems, such as beam and frame. Rogers and Lee [7], and Holden [8] got the deflections of the viscoelastic cantilever under constant uniform load and constant concentrated load, respectively. Yang and Lianis [9] solved viscoelastic beams and frames by the finite element method with a bar finite element. The geometrical nonlinearity is accounted for a mid-point-tangent incremental approach together with coordinate transformation at every step. But this method is difficult to extend into two- and three-dimensional viscoelastic large deformation problems.

From the general continuum mechanics principles, the authors have solved linear viscoelastic large deformation problems by using the U.L. approach [10, 11]. Since the incremental constitutive equation represented by Kirchhoff stress increment tensors and Green strain increment tensors must be transformed to an alternate form expressed by updated Kirchhoff stress increment tensors and updated Green strain increment tensors, the continued equilibrium equation in the U.L. approach is rendered rather complicated. But in the T.L. approach the constitutive equation represented by Kirchhoff stress increment tensors and Green strain increment tensors can be applied directly, so the continued equilibrium is rather simple. In addition, the T.L. approach can avoid modifying the nodal coordinate after every increment step, therefore the computer time can be saved. These are reasons why the T.L. approach arouses more interest for viscoelastic large deformation problems and these will be introduced in this paper.

Using the nonlinear viscoelastic constitutive equation and based upon the virtual work principle of T.L. and U.L. approaches, respectively, the finite element equations of the three-dimensional nonlinear viscoelastic large deformation problem are derived in this paper. The results of viscoelastic cantilever beam are just the same with those in Ref. [11]. The calculation confirms that so long as the constitutive relation is identical, the results calculated by both approaches are the same. The computational results of large deformation nonlinear viscoelastic cantilever and a hollow thick viscoelastic cylinder with a steel casing are in reasonable agreement with Refs [9, 10]. The effects of material incompressibility on stress analysis are discussed.

2. THE INCREMENTAL VARIATIONAL EQUATIONS OF T.L. AND U.L. APPROACHES

As the incremental theory is used to analyse the solid deformation, the formulation begins by dividing the loading path of the solid body problem into a number of equilibrium states, such as $\Omega^{(0)}, \ldots, \Omega^{(N)}, \Omega^{(N+1)}, \ldots$. $\Omega^{(0)}$ is the initial state of the deformation, $\Omega^{(N)}, \Omega^{(N+1)}$ are two intermediate neighbouring states. Let the rectangular cartesian coordinates of the position of the point in $\Omega^{(0)}$, $\Omega^{(N)}$ and $\Omega^{(N+1)}$ states be represented by x_i, X_i and Y_i, $i = 1, 2, 3$ respectively.

Base on the T.L. and U.L. approaches in the equilibrium state $\Omega^{(N+1)}$, we can obtain the virtual work equations, respectively, as follows [12]:

$$\iiint_v \{\Delta S_{ij}\delta\Delta\epsilon_{ij} + S_{ij}\delta(\tfrac{1}{2}\Delta u_{k,i}\Delta u_{k,j}) - \Delta\bar{P}_i\delta\Delta u_i + [S_{ij}\delta\Delta\epsilon_{ij} - \bar{P}_i\delta\Delta u_i]\}\,dv^{(0)} - \iint_{S_\sigma}(\Delta\bar{T}_i + \bar{T}_i)\delta\Delta u_i\,ds^{(0)} = 0 \tag{1}$$

$$\iiint_v \{\Delta^* S_{ij}\delta\Delta^*\epsilon_{ij} + \sigma_{ij}\delta(\tfrac{1}{2}\Delta u_{k,i}\Delta u_{k,j}) - \Delta\bar{P}_i\delta\Delta u_i + [\sigma_{ij}\delta\Delta^*\epsilon_{ij} - \bar{P}_i\delta\Delta u_i]\}\,dv^{(N)} - \iint_{S_\sigma}(\Delta\bar{T}_i + \bar{T}_i)\delta\Delta u_i\,ds^{(N)} = 0, \tag{2}$$

where S_{ij} and ΔS_{ij} are the Kirchhoff stress tensor and its increment; $\Delta\epsilon_{ij}$ is Green strain increment tensor, which has omitted the product of the displacement increments; P_i and $\bar{T}_i$ are body force and surface force on S_σ, which are referred to the initial state $\Omega^{(0)}$. In eqn (2), $\Delta^* S_{ij}$ and $\Delta^*\epsilon_{ij}$ are the updated Kirchhoff stress increment tensor and updated Green strain increment tensor, only the product of displacement increments has been omitted in the $\Delta^*\epsilon_{ij}$; σ_{ij} is the Euler stress tensor, and the body force $\bar{P}_i$ and the surface force on S_σ are defined to the $\Omega^{(N)}$ state.

3. CONSTITUTIVE EQUATION

The large strain capability of many solid propellants and similar materials requires that the stress–strain relation should be formulated in terms of the appropriate stress and strain tensors. The convolution must be so written that the stress in a material element depends on the deformation history of that element. This is most easily handled by means of a Lagrangian analysis using symmetric Kirchhoff stress tensors and Green strain tensors, as both measures consider a material element referred to a specific reference frame that is usually taken as the original unstressed configuration. This substitution of Lagrangian variables was first introduced by Christenson [13] and then employed in the hereditary integral model by Swanson and Christenson [14]. For the multiaxial stress condition it may be given as follows:

$$\{S_{ij}\} = g(\epsilon)\int_0^t E(\xi - \xi')[A]\frac{\partial\{\bar{e}_{pq}\}}{\partial\tau}\,d\tau, \tag{3}$$

where the $g(\epsilon)$ is the strain softening (or pressure-hardening) function which seems to successfully correct the discrepancy between experimental data and those predicted by linear viscoelasticity.

The matrix $[A]$ in the three-dimensional problem is expressed by

$$[A] = \frac{1-\nu}{(1+\nu)(1-2\nu)}\begin{bmatrix} 1 & \frac{\nu}{1-\nu} & \frac{\nu}{1-\nu} & & & \\ & 1 & \frac{\nu}{1-\nu} & & 0 & \\ & & 1 & \frac{1-2\nu}{2(1-\nu)} & & \\ & \text{(SYM)} & & & \frac{1-2\nu}{2(1-\nu)} & \\ & & & & & \frac{1-2\nu}{2(1-\nu)} \end{bmatrix} \tag{4}$$

and $\bar{\epsilon}_{pq} = \epsilon_{pq} - \delta_{pq}\alpha\Delta T$. In eqn (3) we assume the Poisson's ratio ν is nearly constant, as pointed out by Schapery [15].

For the thermorheologically simple materials, the reduced time ξ is given by

$$\xi = \int_0^t \frac{d\eta}{a_T(\eta)}, \quad \xi' = \int_0^\tau \frac{d\eta}{a_T(\eta)}. \tag{5}$$

Let the extension modulus be described by a Prony series as

$$E(t) = \sum_{k=1}^{m} E_k \exp(-\alpha_k t). \tag{6}$$

If we define the convolution at a particular time t_n as

$$\{(S_{ij})_{n,k}\} = g_n(\epsilon)\int_0^{t_n} E_k \exp[-\alpha_k(\xi_n - \xi)][A]\frac{\partial\{\bar{e}_{pq}\}}{\partial\tau}\,d\tau \tag{7}$$

and

$$\{S_{ij}(t_n)\} = \sum_{k=1}^{m}\{(S_{ij})_{n,k}\} \tag{8}$$

then a recursion relation can be easily developed to compute $\{(S_{ij})_{n,k}\}$

$$\{(S_{ij})_{n,k}\} = g_n(\epsilon)\exp(-\alpha_k B_n \Delta t_n)\{(S_{ij})_{n-1,k}\} + g_n(\epsilon)\frac{E_k[1-\exp(-\alpha_k \bar{B}_n\Delta t_n)][A]\{\Delta\bar{e}_{pq}\}}{(\alpha_k \bar{B}_n \Delta t_n)}. \tag{9}$$

Considering the $g_n(\epsilon) = g_{n-1}(\epsilon) + \Delta g_n(\epsilon)$, we can get the Kirchhoff stress increments at the interval Δt_n as follows:

$$\{(\Delta S_{ij})_{n,k}\} = g(\epsilon)\frac{E_k[1-\exp(-\alpha_k\bar{B}_n\Delta t_n)][A]\{\Delta\bar{e}_{pq}\}}{(\alpha_k\bar{B}_n\Delta t_n)} - (g_{n-1}(\epsilon)[1-\exp(-\alpha_k B_n\Delta t_n)] - \Delta g_n(\epsilon)\exp(-\alpha_k B_n\Delta t_n))\{(S_{ij})_{n-1,k}\} \tag{10}$$

where

$$B_n = 1/a_T(t_n)$$

and

$$\bar{B}_n = \left(\frac{t_{n-1}}{t_n}\right)\bar{B}_{n-1} + \left(\frac{\Delta t_n}{t_n}\right)B_n.$$

The first term on the right side represents the stress increments produced by the strain increments at the interval Δt_n, and the second term expresses the relaxation stresses. Obviously, when we calculate the displacement increments at time t_n, the function $\Delta g(\epsilon)$ at time t_n with $\Delta g(\epsilon)$ at time t_{n-1} carries on a modification repeatedly. The computational practice shows that the substitution of $\Delta g(\epsilon)$ at time t_{n-1} for $\Delta g(\epsilon)$ at time Δt_n produces only a small influence on results.

4. CONTINUED EQUILIBRIUM EQUATION

Substituting eqn (10) into eqn (1), we may obtain the continued equilibrium equation of nonlinear viscoelastic large deformation problems by use of the T.L. approach as follows:

$$\iiint_V \{g_n(\epsilon)[C](\Delta\epsilon_{pq} - \delta_{pq}\alpha\Delta T)\delta\Delta\epsilon_{ij} + \tfrac{1}{2}S_{ij}\delta(\Delta u_{i,j}\Delta u_{i,j}) - \sum_k\{(S_{ij})_{n-1,k}\} \times \{g_{n-1}(\epsilon)[1-\exp(-\alpha_k B_n\Delta t_n)] - \Delta g_n(\epsilon)\exp(-\alpha_k B_n\Delta t_n)\}\delta\Delta\epsilon_{ij} + [S_{ij}\delta\Delta\epsilon_{ij} - \bar{P}\delta_i\Delta u_i]\}\,dv^{(0)} - \iint_{S_\sigma}(\Delta\bar{T}_i + \bar{T}_i)\delta\Delta u_i\,ds^{(0)} = 0 \tag{11}$$

where

$$[C] = \left(\sum_k \frac{E_k[1-\exp(-\alpha_k\bar{B}_n\Delta t_n)]}{\alpha_k\bar{B}_n\Delta t_n}\right)[A]. \tag{12}$$

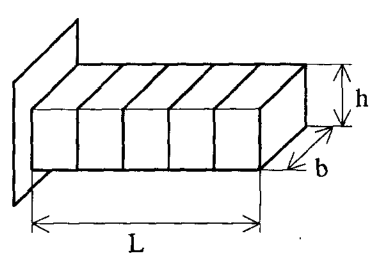

Fig. 1. Cantilever beam.

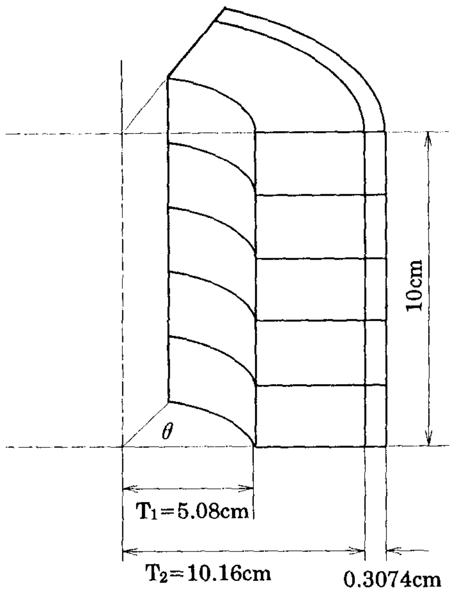

Fig. 2. Deflections of a cantilever under constant uniform load $(ql^3/E(0)I) = \pi/3$ (l—large deformation, f—large deformation and strain softening).

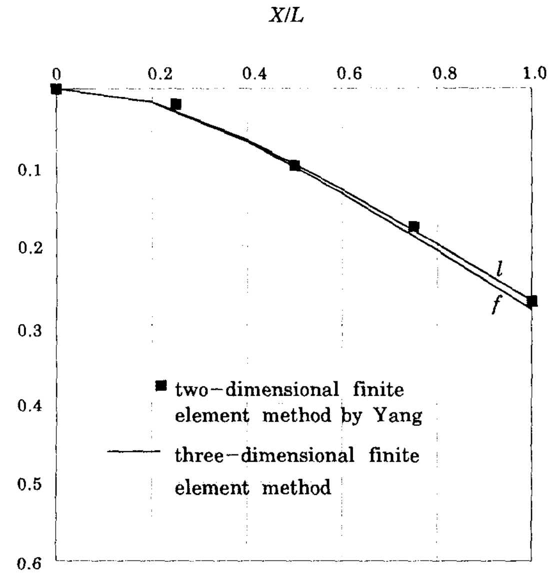

Fig. 3. Deflections of a cantilever under constant concentrated load $(Pl^3/E(0)I) = \pi/3$ (s—small deformation, l—large deformation, f—large deformation and strain softening).

Substituting the relations between $\Delta^* S_{ij}$ and ΔS_{ij} as well as $\Delta^*\epsilon_{ij}$ and $\Delta\epsilon_{ij}$ [12] and eqn (10) into eqn (2), we can also write the continued equilibrium equation of the nonlinear viscoelastic large deformation by use of the U.L. approach in the following form:

$$\iiint_v \Big\{ g_n[C] \frac{1}{D^{(N)}} \frac{\partial X_i}{\partial x_r} \frac{\partial X_j}{\partial x_s} \frac{\partial X_p}{\partial x_c} \frac{\partial X_q}{\partial x_d} \Delta^*\bar{\epsilon}^*_{pq} \delta\Delta^*\epsilon_{ij}$$

$$+ \tfrac{1}{2}\sigma_{ij}\delta(\Delta u_{l,i}\Delta u_{l,j})$$

$$- \sum_k \{(S_{rs})_{n-1,k}\}\{g_{n-1}(\epsilon)[1-\exp(-\alpha_k B_n \Delta t_n)]$$

$$- \Delta g_n(\epsilon)\exp(-\alpha_k B_n \Delta t_n)\} \frac{1}{D^{(N)}} \frac{\partial X_i}{\partial x_r} \frac{\partial X_j}{\partial x_s} \delta\Delta^*\epsilon_{ij}$$

$$+ [\sigma_{ij}\delta\Delta^*\epsilon_{ij} - \bar{P}_i\delta\Delta u_i] - \Delta\bar{P}_i\delta\Delta u_i \Big\} \mathrm{d}v^{(N)}$$

$$- \iint_{S_\sigma} (\Delta\bar{T} + \bar{T})\delta\Delta u_i \,\mathrm{d}s^{(N)} = 0. \qquad (13)$$

If the effects of changing temperature and strain-softening function are not taken into consideration, namely $\bar{B}_n = B_n = 1$, and $g(\epsilon) = 1$, $\Delta g(\epsilon) = 0$, eqn (13) is simplified to eqn (16) in Ref. [11].

5. THE FINITE ELEMENT FORMULATION

By using the 20-node three-dimensional isoparametric element and considering the relaxation stress and temperature stress as initial stresses, the finite element formulae may be derived from eqns (11) and (13), respectively:

$$\{g_n(\epsilon)([K_0]+[K_u]) + [K_s]\}\{\Delta u\}$$
$$= \{\Delta Q\} + \{\Delta E\} + \{\Delta I\} + \{\Delta T\} \qquad (14)$$

Table 1. Deflections calculated by three-dimensional isoparametric element under the concentrated load $(-W/L)$

Time (h)	Approach	x/l 0.2	0.4	0.6	0.8	1.0
0	T.L.	0.01591	0.06392	0.13729	0.22736	0.32577
	U.L.	0.01591	0.06392	0.13729	0.22736	0.32577
1	T.L.	0.01703	0.06793	0.14464	0.23768	0.33892
	U.L.	0.01703	0.06793	0.14465	0.23770	0.33894
10	T.L.	0.02227	0.08835	0.18754	0.30742	0.43799
	U.L.	0.02227	0.08836	0.18754	0.30742	0.43799
20	T.L.	0.02532	0.09999	0.21164	0.34613	0.49255
	U.L.	0.02532	0.09999	0.21164	0.34613	0.49255

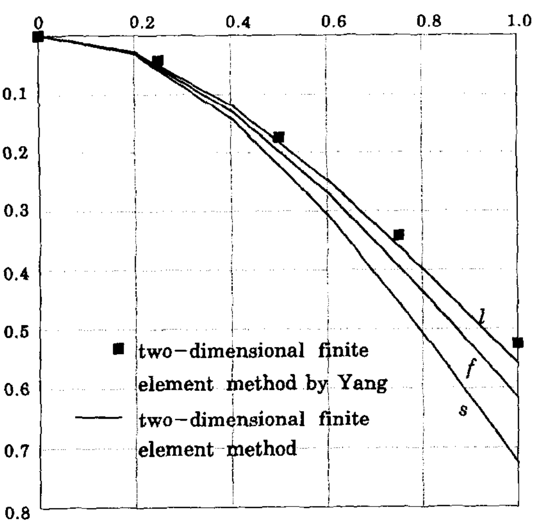

Fig. 4. A hollow thick viscoelastic cylinder with a steel casing.

$$\{g_n(\epsilon)[K]+[K_G]\}\{\Delta u\}$$
$$=\{\Delta Q'\}+\{\Delta E'\}+\{\Delta I'\}+\{\Delta T'\}. \quad (15)$$

The form of the matrix $[K_G]$ in the three-dimensional problem was described in Ref. [11]. The discrepancy between eqn (15) and eqn (17) in Ref. [11] is that eqn (15) includes strain softening function and a time–temperature shift factor.

In eqn (14), $[K_0]$ represents the stiffness matrix of a small deformation. $[K_u]$ and $[K_s]$ are initial displacement and initial stress matrices, which consider effects of large deformation and are given by

$$[K_u]^e=\int_{-1}^{1}\int_{-1}^{1}\int_{-1}^{1}([B_0]^T[C][B_L]+[B_L]^T[C][B_L]$$
$$+[B_L]^T[C][B_0])|J|\,\mathrm{d}\xi\,\mathrm{d}\eta\,\mathrm{d}\zeta \quad (16)$$

$$[K_s]^e=\int_{-1}^{1}\int_{-1}^{1}\int_{-1}^{1}[G]^T[M][G]|J|\,\mathrm{d}\xi\,\mathrm{d}\eta\,\mathrm{d}\zeta,$$

where the matrices $[G]$ and $[M]$ are given in the Appendix. In the terms of the right side of eqn (14), $\{\Delta Q\}$ and $\{\Delta E\}$ represent the nodal forces produced by load increments and non-equilibrium residual, respectively, and $\{\Delta I\}$ and $\{\Delta T\}$ express the nodal forces induced by relaxation stress and temperature stress and may be described, respectively, as follows:

$$\{\Delta I\}=\int_{-1}^{1}\int_{-1}^{1}\int_{-1}^{1}([B_0]+[B_L])^T\Big\{\sum_k\{(S_{ij})_{n-1,k}\}$$
$$\times\{g_{n-1}(\epsilon)[1-\exp(-\alpha_k B_n\Delta t_n)]$$
$$-\Delta g_n(\epsilon)\exp(-\alpha_k B_n\Delta t_n)\}\Big\}|J|\,\mathrm{d}\xi\,\mathrm{d}\eta\,\mathrm{d}\zeta \quad (17)$$

and

$$\{\Delta T\}=\int_{-1}^{1}\int_{-1}^{1}\int_{-1}^{1}([B_0]+[B_L])^T g_n(\epsilon)$$
$$\times[C]\delta_{pq}\alpha\Delta T|J|\,\mathrm{d}\xi\,\mathrm{d}\eta\,\mathrm{d}\zeta. \quad (18)$$

In accordance with the above-mentioned two approaches, the programs of three-dimensional nonlinear viscoelastic large deformation with 14 and eight Gauss integration points have been written. The latter is suitable only for the stress analysis of nearly incompressible solids.

Table 2. Distribution of radial stresses at large deformation ($-\sigma_r/p_0$)

	r/r_2							
	0.5625		0.6875		0.8125		0.9375	
	Deformation situation							
Time (h)	2-D	3-D	2-D	3-D	2-D	3-D	2-D	3-D
0.0	0.8803	0.8612	0.7410	0.7295	0.6612	0.6532	0.6124	0.6058
1.0	0.9006	0.8783	0.7759	0.7577	0.7044	0.6885	0.6596	0.6453
1.5	0.9043	0.8811	0.7843	0.7644	0.7155	0.6974	0.6724	0.6556
2.0	0.9070	0.8827	0.7904	0.7688	0.7236	0.7034	0.6817	0.6625

Table 3. Distribution of tangential stresses at large deformation ($-\sigma_\theta/p_0$)

	r/r_2							
	0.5625		0.6875		0.8125		0.9375	
	Deformation situation							
Time (h)	2-D	3-D	2-D	3-D	2-D	3-D	2-D	3-D
0.0	0.0300	0.0438	0.1706	0.1850	0.2584	0.2646	0.3095	0.3142
1.0	0.1292	0.1385	0.2652	0.2659	0.3410	0.3377	0.3878	0.3824
1.5	0.1566	0.1635	0.2904	0.2876	0.3645	0.3575	0.4100	0.4008
2.0	0.1754	0.1803	0.3084	0.3024	0.3816	0.3709	0.4262	0.4134

Table 4. Stresses (σ_r/p_0) in a hollow thick incompressible viscoelastic cylinder with a casing ($E = 7037\,e^{-0.8889t}$ MPa, $\nu = 0.499$, $E_c = 2.111$ GPa, $\nu_c = 0.3015$, $p_0 = 3$ MPa)

Time (h)	Solution	r/r_2 0.5625	0.6895	0.8125	0.9375
	Exact	0.7292	0.3921	0.1983	0.0767
0.0	8-GIP	0.7005	0.3770	0.1922	0.0768
	14-GIP	−0.1191	0.0108	0.0016	−0.0255
	Exact	0.7300	0.3939	0.2006	0.0793
0.1	8-GIP	0.7017	0.3797	0.1957	0.0807
	14-GIP	−0.1144	0.015	0.0059	−0.0211
	Exact	0.7331	0.4008	0.2100	0.0898
0.5	8-GIP	0.7068	0.3902	0.2092	0.0962
	14-GIP	−0.0957	0.0302	0.0226	−0.0040
	Exact	0.7369	0.4093	0.2209	0.1027
1.0	8-GIP	0.7130	0.4030	0.2259	0.1152
	14-GIP	−0.0728	0.0518	0.0430	0.0171

Table 5. Stresses (σ_r/p_0) in a hollow thick nearly-incompressible viscoelastic cylinder ($\nu = 0.499$) with different casing (1 h)

E_c (GPa)	Solution	r/r_2 0.5625	0.6875	0.8125	0.9375
	Exact	0.7369	0.4093	0.2209	0.1027
2.111	8-GIP	0.7130	0.4030	0.2259	0.1152
	14-GIP	−0.0728	0.0518	0.0430	0.0171
	Exact	0.9674	0.9268	0.9034	0.8887
211.1	8-GIP	0.9734	0.9445	0.9281	0.9178
	14-GIP	0.8997	0.9113	0.9104	0.9082

6. NUMERICAL RESULTS AND DISCUSSION

(1) *Cantilever beam under constant concentrated load at the free end*

For checking the correctness of eqn (11) and the program, the viscoelastic material, delrin acetal resin, is chosen in the calculation. This material was used by Rogers and Lee [7], Yan and Lianis [9], as well as the authors [10, 11] for numerical examples. The relaxation modulus $E(t)$ can be deduced from the experimental curves as follows:

$$\frac{E(t)}{E(0)} = 0.468545\,e^{-0.000035726t} + 0.53155\,e^{-0.1170t}. \tag{19}$$

The beam shown in Fig. 1 is divided uniformly by five elements, and its Poisson's ratio is assumed to be 0.4. The deflections on the bottom surface are calculated by the T.L. approach from 0 to 20 h and are shown in Table 1, in which the results of the U.L. approach are taken from Ref. [11].

The computational results confirm the conclusion first proposed by Bathe *et al.* [16] that, so long as the constitutive equation is identical, the final results calculated by both approaches are the same. As the constitutive equation is represented by Kirchhoff stress tensors and Green strain tensors, such as the viscoelastic large deformation situation, the T.L. approach not only simplifies the continued equilibrium equation, but also avoids modifying the nodal coordinate after each incremental step, thus computer time may be saved.

(2) *Cantilever with the strain-softening effect*

Applying the T.L. approach and using the strain-softening function $g(\epsilon)$ taken from Ref. [14], we compute the large deflections of a nonlinear viscoelastic cantilever under constant uniform load and constant concentrated load, respectively. The deflection curves are shown in Figs 2 and 3 and the results obtained by Yang and Lianis [9] are provided for comparison. It is rational that the strain-softening effect causes the increase of deflection, and the greater the deformation of cantilever, the more remarkable the softening effects become.

(3) *A hollow thick viscoelastic cylinder with a steel casing under uniform internal pressure*

The geometry of a hollow thick viscoelastic cylinder with a steel casing is shown in Fig. 4. The top and bottom surfaces are fixed and uniform internal pressure p_0 is taken as 3 MPa. To decrease the

Table 6. Stress (σ_r/p_0) in a hollow nearly-incompressible viscoelastic cylinder of different Poisson's ratio with a steel casing (1 h)

ν	Solution	r/r_2 0.5625	0.6875	0.8125	0.9375
0.5	Exact	0.9674	0.9268	0.9034	0.8887
0.4999	8-GIP	0.9750	0.9478	0.9323	0.9227
	14-GIP	0.2841	0.6369	0.7684	0.8328
0.499	8-GIP	0.9734	0.9445	0.9281	0.9178
	14-GIP	0.8997	0.9113	0.9104	0.9082

computational workload, we take only a sector region $\theta = 15^\circ$ in the calculation and divide it into 25 element and 228 nodes. The viscoelastic behaviour can be expressed by a Maxwell model.

The relaxation modulus E and Poisson's ratio v are, respectively, $E = 703.7\,e^{-0.88889t}$ MPa, $v = 0.4$. The outer steel casing has the properties $E_c = 211.1$ GPa, $v_c = 0.3015$. For lack of better information, the pressure hardening function $g(\epsilon)$ was taken as unity.

The exact solution and results of this work in a small deformation situation are in good agreement. The radial and tangential stresses evaluated by the T.L. approach in the large deformation situation are shown in Tables 2 and 3, in which the values of stress in a two-dimensional large deformation situation are taken from Ref. [10].

It can be found that the radial and tangential stresses in the viscoelastic cylinder increase gradually along with the increase in time. The trend that the stresses in the viscoelastic cylinder approach the internal pressure along with the increase of time in the plane-strain situation is slightly stronger than that in the three-dimensional deformation situation.

For the stress analysis of nearly incompressible viscoelastic solid, a code had been developed by Yadagiri and Reddy [17], using isoparametric elements with selective integration procedure, which is a third-order Gauss rule for deviatoric response and second-order Gauss rule for volumetric response. In the present work, according to the form of the constitutive eqn (3), in which the material response is not separated into shearing and volumetric components, reduced numerical integration is employed for computing the element stiffness matrices and then the general formulation is simpler than Ref. [17]. The results obtained using eight and 14 Gauss integration points (GIP) along with the closed form solution (exact solution for $v = 0.5$) are given in Table 4. It is seen from Table 4 that the present work also gives good results for nearly incompressible viscoelastic structure, and it can be found from Table 5 that, along with increase of modulus of casing, although the stress values from using 14 Gauss integration points approach exact values, the regularity of stress distribution along the radial direction is still wrong.

Along with the increase of Poisson's ratio v of viscoelastic nearly-incompressible materials, not only the regularity of radial stress distribution but also the stress values, which are obtained by 14 Gauss integration points and shown in Table 6, are incorrect, and the maximum error of the radial stresses obtained by eight Gauss integration points is less than 4%.

7. CONCLUSION

In the analysis of viscoelastic large deformation problems, the T. L. approach not only simplifies the continued equilibrium equation, but also avoids modifying the nodal coordinate after each incremental step, thus computer time may be saved.

Complex nonlinear viscoelastic behaviour represented by strain softening function $g(\epsilon)$ can easily be completed in the finite element method. Results confirm that the larger the deformation of viscoelastic solid, the larger the effect of its strain-softening.

For the stress analysis of a nearly incompressible viscoelastic solid, the use of reduced integration in the calculation of element stiffness matrices has proved to lead to a dramatic improvement in results.

REFERENCES

1. O. C. Zienkiewicz and M. Wattson, Some creep effects in stress analysis with particular reference to concrete pressure vessels. *Nucl. Engng Des.* **4,** 406–412 (1966).
2. O. C. Zienkiewicz, M. Wattson and I. P. King, A numerical method of visco-elastic stress analysis. *Int. J. Mech. Sci.* **10,** 807–827 (1968).
3. J. L. White, Finite elements in linear viscoelasticity. *Proc. 2nd Conf. Matrix Methods in Structural Mechanics*, pp. 489–516 (1968).
4. J. H. Argyris, K. S. Pister, J. Szimmat and K. J. William, Unified concepts of constitutive modelling and numerical solution methods for concrete creep problems. *Comput. Meth. Appl. Mech. Engng* **10,** 197–246 (1977).
5. H. R. Srinathe and R. W. Lewis, A finite element method for thermoviscoelastic analysis of plane problems. *Comput. Meth. Appl. Mech Engng* **25,** 21–23 (1981).
6. R. A. Adey and C. A. Brebbia, Efficient method for solution of viscoelastic problems. *J. Engng Mech.* **99–6,** 1119–1127 (1973).
7. T. G. Rogers and E. H. Lee, On the finite deflection of a viscoelastic cantilever. *Proc. 4th U.S. Natl Cong. of Applied Mechanics*, ASME, pp. 977–987 (1962).
8. J. T. Holden, On the finite deflection of thin viscoelastic beams. *Int. J. Numer. Meth. Engng* **5,** 271–275 (1972).
9. T. Y. Yang and G. Lianis, Large displacement analysis of viscoelastic beams and frames by the finite element method. *J. Appl. Mech.* **41,** 635–640 (1974).
10. Y. P. Shen, Y. H. Chen and Y. F. Pen, The finite element method of viscoelastic large deformation plane problem with Kirchhoff stress tensors–Green strain tensors constitutive relation. *Acta Mech. Solida Sinica* **1,** 235–248 (1988).
11. Y. P. Shen, J. J. Yin and S. C. Chen, The analysis of three-dimensional viscoelastic large deformation problems by using U. L. approach. *Comput. Struct. Mech. Appl.* (in Chinese) **2,** 43–54 (1987).
12. K. Washizu, *Variational Method in Elasticity and Plasticity*. Pergamon Press, Oxford (1982).
13. R. M. Christenson, A nonlinear theory of viscoelasticity for application to elastomers. *J. Appl. Mech.* **47,** 762–768 (1980).
14. S. R. Swason and L. W. Christenson, A constitutive formulation for high-elongation propellants. *J. Spacecraft* **20,** 559–566 (1983).
15. R. A. Schapery, A theory of crack initiation and growth in viscoelastic media I. Theoretical development. *Int. J. Fracture* **11,** 141–159 (1975).
16. K. J. Bathe, E. Ramm and E. L. Wilson, Finite element formulations for large deformation dynamic analysis. *Int. J. Numer. Meth. Engng* **9,** 353–386 (1975).
17. S. Yadagiri and C. P. Reddy, Viscoelastic analysis of nearly incompressible solids. *Comput. Struct* **20,** 817–825 (1985).

APPENDIX

The matrices $[G]$ and $[M]$ are

$$[G] = \begin{bmatrix} \frac{\partial N_1}{\partial x} & & & & \frac{\partial N_{20}}{\partial x} & 0 & 0 \\ \frac{\partial N_1}{\partial y} & 0 & 0 & \cdots & \frac{\partial N_{20}}{\partial y} & & \\ \frac{\partial N_1}{\partial z} & & & & \frac{\partial N_{20}}{\partial z} & & \\ & \frac{\partial N_1}{\partial x} & & & & \frac{\partial N_{20}}{\partial x} & \\ 0 & \frac{\partial N_1}{\partial y} & 0 & \cdots & 0 & \frac{\partial N_{20}}{\partial y} & 0 \\ & \frac{\partial N_1}{\partial z} & & & & \frac{\partial N_{20}}{\partial z} & \\ & & \frac{\partial N_1}{\partial x} & & & & \frac{\partial N_{20}}{\partial x} \\ 0 & 0 & \frac{\partial N_1}{\partial y} & \cdots & 0 & 0 & \frac{\partial N_{20}}{\partial y} \\ & & \frac{\partial N_1}{\partial z} & & & & \frac{\partial N_{20}}{\partial z} \end{bmatrix} \tag{A1}$$

and

$$[M] = \begin{bmatrix} [S] & 0 & 0 \\ 0 & [S] & 0 \\ 0 & 0 & [S] \end{bmatrix} \tag{A2}$$

where

$$[S] = \begin{bmatrix} S_{11} & S_{12} & S_{13} \\ S_{21} & S_{22} & S_{23} \\ S_{31} & S_{32} & S_{33} \end{bmatrix}. \tag{A3}$$